Vision Research 188 (2021) 234–245

Contents lists available at ScienceDirect

Vision Research

journal homepage: www.elsevier.com/locate/visres

A multiplicity of color-responsive cortical mechanisms revealed by the dynamics of cVEPs

Valerie Nunez [a,*], James Gordon [b,a], Robert M. Shapley [a]

[a] Center for Neural Science, New York University, 4 Washington Place, New York, NY 10003, USA
[b] Psychology Department, CUNY Hunter College, 695 Park Ave, New York, NY 10065, USA

ARTICLE INFO

Keywords:
Color
Human
Visual cortex
Cone-contrast
Transientness

ABSTRACT

Our results connect higher-order color mechanisms deduced from psychophysics with the known diversity of populations of double-opponent, color-responsive cells in V1. We used the chromatic visual evoked potential, the cVEP, to study responses in human visual cortex to equiluminant color patterns. Stimuli were modulated along three directions in color space: the cardinal directions, L-M and S, and along the line in color space from the white point to the color of the Red LED in the display screen (the Red direction). The Red direction is roughly intermediate between L-M and S in DKL space in cone-contrast coordinates. While cVEP response amplitude, latency, and width–and their dependences on cone contrast– were similar in the L-M and Red directions, the Transientness of the Red response was significantly greater than for responses to stimuli in the L-M direction and in the S direction. This difference in response dynamics supports the concept that there are multiple, distinct neuronal populations, so-called higher- order color mechanisms, for color perception within human V1 cortex.

1. Introduction

Color perception depends on postreceptoral cone-opponent interactions (Hurvich & Jameson, 1957; DeValois, 1960). In the retina and Lateral Geniculate Nucleus (LGN) there are two distinct populations of cone-opponent cells: cells that compute the difference between L (565 nm) and M (535 nm) cone activations, in the Parvocellular pathway; and cells that compute the difference between S (440 nm) vs L and M cones in the Koniocellular pathway (Casagrande, 1994; Chatterjee & Callaway, 2003). These two pathways correspond to the cardinal directions in the DKL color space (Derrington, Krauskopf, & Lennie, 1984; Krauskopf, Williams, & Heeley, 1982; MacLeod & Boynton, 1979). However, adaptation experiments (e.g., Krauskopf & Gegenfurtner, 1992; Webster & Mollon, 1994) and masking experiments (e.g., Bouet & Knoblauch, 2004; Gegenfurtner & Kiper, 1992) reveal the existence of neural mechanisms tuned to colors not in the cardinal directions. Furthermore, there is neurophysiological evidence (from single-cell recordings in the primary visual cortex, V1, of Macaque monkeys) for color-responsive cells that prefer non-cardinal directions (Lennie, Krauskopf, & Sclar, 1990) or that receive cone inputs that would make them prefer non-cardinal colors (Johnson, Hawken, & Shapley, 2004). However, it is not known at what cortical level the higher-order color mechanisms (Krauskopf et al., 1986) are represented in humans.

In this paper, our experimental results on the dynamics of responses to different color directions suggest the existence of higher-order color mechanisms in human visual cortex as early as V1, consistent with prior results on single-unit recording in Macaque V1 (Lennie et al., 1990; Johnson et al., 2004). The experiments reported here focused on neural activity in human early visual cortex, recorded with electrophysiological techniques. Neurophysiological study of single cells in primate V1 shows that V1 transforms color signals (Thorell, DeValois, & Albrecht, 1984; Lennie et al., 1990; Johnson, Hawken, & Shapley, 2001; Conway et al., 2010), rather than having all color computations deferred until later in the cortex (Zeki, 1983). Single-neuron studies indicated similar properties of edge-dependent color-selective cells in Macaque V1 and V2 (Friedman, Zhou, & von der Heydt, 2003). Results of human psychophysics and neuropsychology imply an early cortical site for color contrast (Hurlbert & Wolf, 2004). Human V1 activity measured by fMRI is modulated strongly by pure color stimuli (Engel, Zhang, & Wandell, 1997; Kleinschmidt, Lee, Requardt, & Frahm, 1996; Mullen, Dumoulin, McMahon, de Zubicaray, & Hess, 2007). More evidence for the involvement of V1 in color perception comes from study of the desaturation of colored targets by brightness contrast (Bimler, Paramei, & Izmailov, 2009; Xing et al., 2015; Faul, Ekroll, & Wendt, 2008). It was

* Corresponding author at: Center for Neural Science, New York University, 4 Washington Place, New York, NY 10003, USA.
E-mail address: valerie.nunez@nyu.edu (V. Nunez).

https://doi.org/10.1016/j.visres.2021.07.017
Received 7 April 2021; Received in revised form 26 July 2021; Accepted 28 July 2021
Available online 10 August 2021

found that a corresponding suppression of response to color by brightness contrast takes place in V1 cortex (Xing et al., 2015). We think color processing is done in V1 because cortical computations of spatial interactions in color perception need to take place where the spatial layout of the scene is preserved – in V1′s precise visuotopic map (Wandell & Winawer, 2011).

We investigated the multiplicity of the types of color-responsive neurons in the primary visual cortex by using the chromatic Visual Evoked Potential, the cVEP, often studied before (Murray, Parry, Carden, & Kulikowski, 1987; Nunez, Shapley, & Gordon, 2017; Rabin, Switkes, Crognale, Schneck, & Adams, 1994; Souza et al., 2008; Xing et al., 2015; Crognale, 2002; Crognale, Duncan, Shoenhard, Peterson, & Berryhill, 2013). Diverse sources of evidence – from lack of attentional effects, and from the sites of lesions that cause cerebral dyschromatopsia – have led others to conclude that the cVEP is an index of V1 responses to color (Highsmith & Crognale, 2010; Victor, Maiese, Shapley, Sidtis, & Gazzaniga, 1989; Crognale et al., 2013).

The optimum stimulus for the cVEP is a chromatic patterned stimulus rather than a spatially uniform field of color (Murray et al., 1987; Nunez, Shapley, & Gordon, 2018; Rabin et al., 1994), and this is true for color stimuli in both the L-M and S color directions (Rabin et al., 1994; cf. **Section 3,** Fig. 3 below). The results on spatial tuning suggest that the pattern cVEP is tapping the activity of spatially-tuned, color responsive neurons of the kind that were found in single-unit studies of Macaque V1 (Thorell et al., 1984; Lennie et al., 1990; Johnson et al., 2001). It should be noted that spatially-tuned, color-responsive neurons (what we have called *double-opponent cells* (Johnson et al., 2004; Shapley et al., 2019) following Livingstone and Hubel (1984)) are the great majority of color-responsive neurons in V1 (Friedman et al., 2003; Johnson et al., 2001). The existence of double-opponent cells was adumbrated by the discovery of spatially-tuned color channels in human psychophysical experiments (Switkes, Bradley, & DeValois, 1988; Bradley, Switkes, & DeValois, 1988).

Previously, Duncan et al. (2012) found evidence for higher-order color mechanisms in the cVEP, using chromatic contrast adaptation. In this study, we present results that support the idea of higher-order color mechanisms in human early visual cortex based on the contrast-dependent dynamics of the cVEP response in different directions in color space.

2. Methods

2.1. Participants

All observers gave informed consent to participate in this study. The experiments were conducted in accordance with the principles embodied in the Declaration of Helsinki and were approved by the Hunter College/City University of New York and the New York University Institutional Review Boards.

A total of 17 observers participated in the study. Of the 15 observers (six male, nine female) aged 20 to 50 ($M = 32.4$, $SD = 12.1$) who viewed stimuli in the Red color direction, 13 provided useable data. Of eight observers (one male, seven female) aged 21 to 51 ($M = 27.3$, $SD = 10.8$) who viewed L-M and S stimuli, seven gave useful data. Six observers participated in both sets of experiments and, of these, four had measurable responses. All participants had normal color vision, assessed with: Pseudo-isochromatic plates; the Farnsworth dichotomous D15 hue test; Lanthony's desaturated 15 hue test; and the Farnsworth-Munsell 100-hue test. The participants also had at least 20/20 (or corrected to 20/20) visual acuity.

2.2. Apparatus

A Sony PVM-A170 OLED monitor was used to present the stimuli. The monitor had a diagonal screen size of 42 cm (effective picture size 365.8 × 205.7 mm, which at the viewing distance of 114 cm corresponded to 18.3° by 10.3° visual angle), resolution of 1920 × 1080 and frame rate of 60 Hz. The screen was calibrated using a Photo Research PR670 Spectrascan Radiometer/Photometer to calculate gamma corrections for the individual red, green and blue LEDs to ensure complete control of intensities on the screen.

2.3. Visual stimuli

Two kinds of color stimuli were used: color checkerboards and uniformly-colored squares. The checkerboard pattern consisted of a small central colored checkerboard surrounded by an area in which the colored checks faded outwards gradually to the background gray of the screen. The central checkerboard was 3.75 cm × 3.75 cm, corresponding to 1.875° x 1.875° of arc and had 8 × 8 checks, giving a dominant spatial frequency of 3.02c/deg, slightly above the peak of the cVEP spatial frequency response reported by Rabin et al. (1994) but well below their recorded cut-off frequencies. Colored squares were also used to study the sensitivity of the cVEP to color stimuli without much spatial structure. These were the same size as the central checkerboards and were also surrounded by a color-fade area. Sample checkerboard and uniform-square stimuli are provided in Fig. 1. For both checkerboards and colored squares, the fading transition from maximum color at the edge of the central square to zero color (i.e. the gray background) occurred as a tanh function, width 3.75 cm. Therefore, including the outer fade-area, there was some degree of color subtending a total angle of 5.625°, though color was reduced by a factor of two within a total angle of 3.75°.

The screen's background color was approximately equivalent to that of equal-energy white. For experiments in the Red direction, the gray background had a luminance of 32.1 cd/m^2, an equivalent color temperature of 5786° and CIE x-y coordinates of (0.326, 0.341). In the L-M and in the S-direction, the background had a luminance of 30.2 cd/m^2, a color temperature of 5790° and CIE coordinates of (0.326, 0.340).

For the Red direction, pattern color was from a range of contrasts along the direction of the Red screen LED. For L-M, and S directions, pattern color was from a range of cone-contrasts in the L-M and S directions of DKL space (Derrington et al., 1984). As all stimuli were equiluminant with the background, there was no luminance modulation. In the L-M direction, excitation of L cones relative to the background is equal and opposite to the excitation of M cones; S-cones are not excited. For S stimuli, the L and M cones are not excited relative to the background; the stimuli are S-cone-isolating. For each checkerboard stimulus, the first check color was in one of the three color directions (Red, L-M or S); the second check was the complement of the first, so that spatially-averaged color over the entire checkerboard was the background gray. To obtain the complement of a color for a participant, it was first ensured that the color was equiluminant with the gray background for the participant (see **Section 2.4**). The complement was then calculated as what would have to be added to the color to result in the background gray. Spatial averaging to the background gray was evident when one stepped away from the screen. When individual checks were no longer discernible, the color-complement checkerboard merged into the gray background. Sample stimuli for each color direction are presented in Fig. 1.

The contrasts of the stimulus colors are presented in Table 1. The L, M and S cone contrasts in the table were calculated as the ratio of differential cone excitation (difference in cone excitation between color and background) divided by the excitation caused by the background. The Koniocellular pathway was driven by S-cone contrast. The excitatory drive for the Parvocellular pathway was L-M contrast as shown in Table 1. For intermediate directions, for instance the Red direction, the magnitude of stimulus contrast was calculated as $\sqrt{(\text{L-M})^2 + \text{S}^2}$, the length of the stimulus vector in a vector space with axes |L-M| and |S|.

Fig. 2 presents the loci of the stimuli in color space. The CIE x-y color coordinates of the stimulus colors, their complements, and the background gray, are presented in Fig. 2A. Color-complement checkerboards

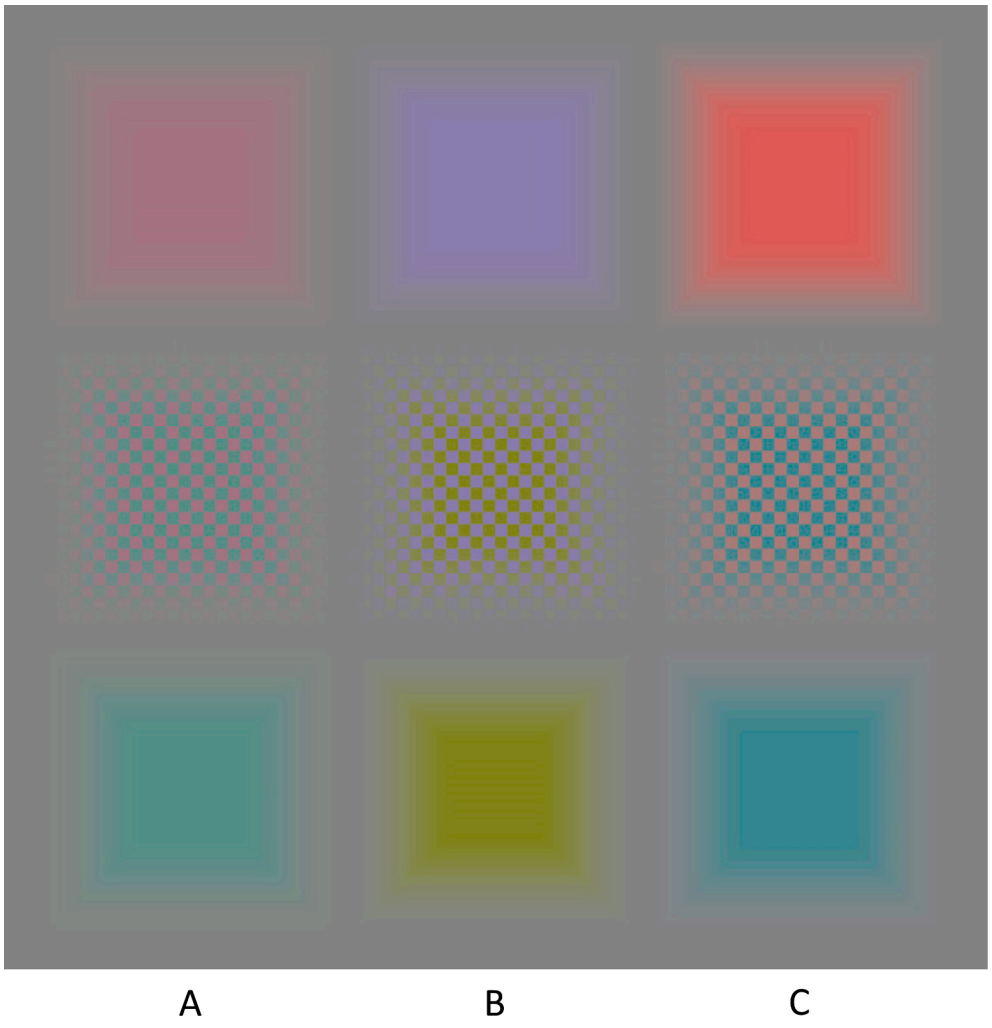

Fig. 1. Sample stimuli that would be centered on the gray background of the screen. In the middle row a central 8x8 checkerboard is surrounded by a checkered region that fades gradually to the background gray. In the top and bottom rows, a uniform colored square of same central size as the checkerboard is surrounded by a colored region that fades gradually to the background gray. In the top row are squares of specific cone contrast in the (A) L-M direction (B) S-cone-isolating direction or (C) Red direction, a color direction between the L-M and S axes. The bottom row shows complements of those colors. The middle row shows checkerboards of color and complement. The central, highest-contrast region of each pattern spanned 1.875° x 1.875°. All colors were equiluminant with the background for each participant. (For interpretation of the references to color in this figure legend, the reader is referred to the web version of this article.)

Table 1
Cone-contrast (defined as differential cone excitation of stimulus color from background gray divided by excitation due to background) and the contrast measures used to describe each stimulus color presented.

	Cone-contrast			Contrast measure		
Color direction	L	M	S	|L-M|	|S|	$\sqrt{(L\text{-}M)^2 + S^2}$
S-cone-isolating	0.003	0.002	0.151	0.000	0.151	0.151
	−0.004	−0.008	0.333	0.004	0.333	0.333
	0.008	0.003	0.480	0.006	0.480	0.480
	0.009	0.006	0.631	0.003	0.631	0.631
	−0.001	−0.009	0.868	0.008	0.868	0.868
L-M	0.015	−0.028	−0.008	0.043	0.008	0.044
	0.036	−0.056	−0.010	0.093	0.010	0.093
	0.045	−0.092	−0.001	0.137	0.001	0.137
	0.054	−0.124	0.002	0.178	0.002	0.178
	0.084	−0.133	−0.011	0.218	0.011	0.218
Red	0.015	−0.035	−0.055	0.050	0.055	0.074
	0.021	−0.053	−0.089	0.075	0.089	0.116
	0.034	−0.079	−0.131	0.113	0.131	0.173
	0.041	−0.097	−0.163	0.138	0.163	0.214
	0.044	−0.116	−0.191	0.160	0.191	0.249
	0.055	−0.129	−0.219	0.183	0.219	0.286
	0.068	−0.148	−0.258	0.216	0.258	0.336

were presented at several different cone-contrast levels up to the maximum possible within the screen's gamut for each color direction. The stimulus colors are also represented in DKL space (Derrington et al., 1984) in cone-contrast coordinates in Fig. 2B. Note that the DKL space in Fig. 2B plots distance along the cardinal directions in cone-contrast coordinates in both the S and L-M directions (Brainard, 1996). While the L-M and S-cone-isolating color directions were chosen to isolate responses from Parvocellular and Koniocellular pathways respectively,

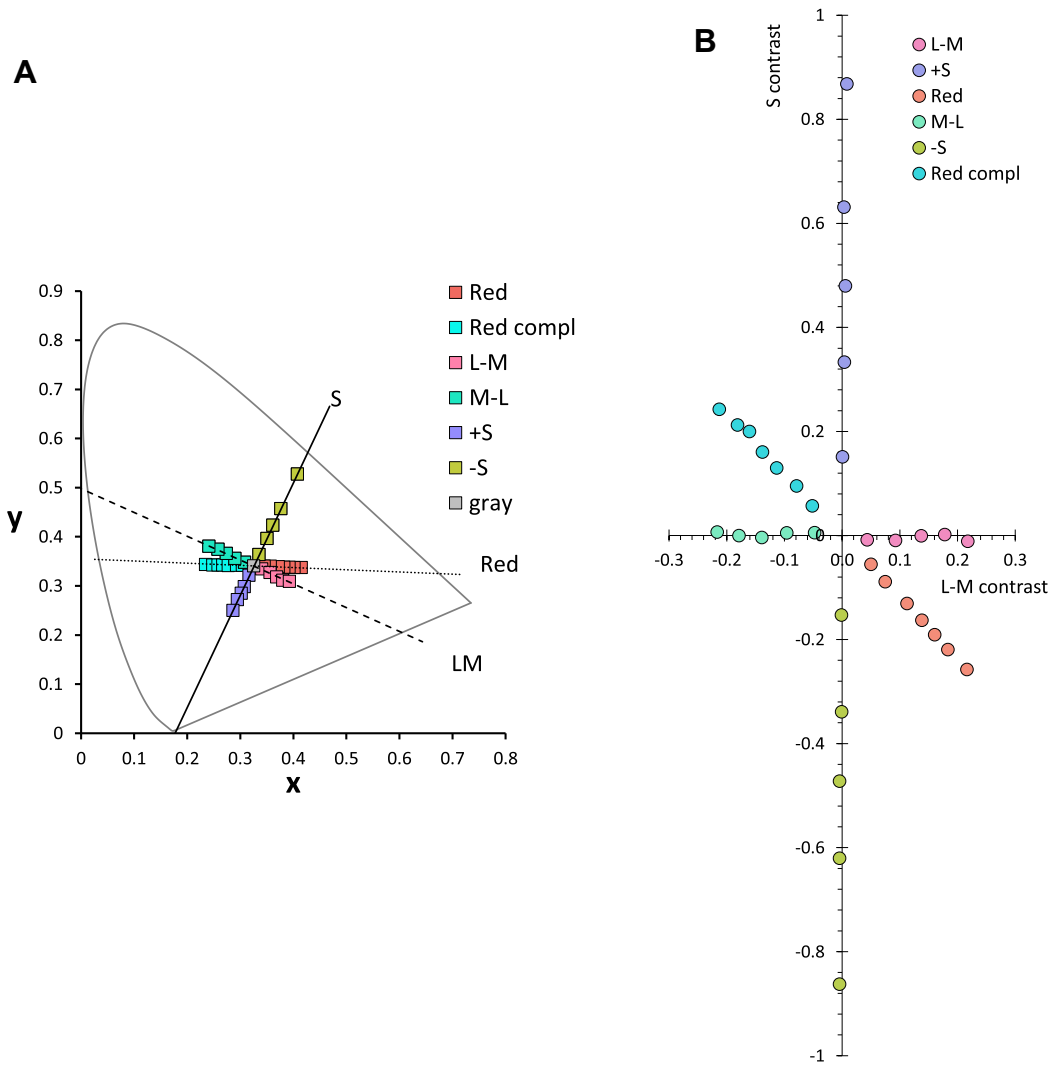

Fig. 2. A. CIE x-y color coordinates of the stimuli used and the background gray. The dashed line labeled LM corresponds to the L-M color direction. The solid line labeled S corresponds to the S-cone-isolating color direction. The dotted line labeled Red corresponds to the color direction of the red primary of the OLED screen. B. Representation of the stimuli in the isoluminant plane of DKL space, in which the distance is in terms of cone-contrast (cf. Brainard, 1996). The x-coordinate is the L-M contrast and the y-coordinate is the S-cone-contrast. (For interpretation of the references to color in this figure legend, the reader is referred to the web version of this article.)

the "Red" color direction was an intermediate color direction corresponding to the color direction of the red primary of the OLED screen. From Fig. 2B it is evident that stimuli along the Red color direction should produce a combination of responses from both L-M and S-cone-driven mechanisms.

For each stimulus, the screen would cycle between the gray background and the color pattern. This cycle was a 0.5 s period of background gray, followed by 0.5 s of pattern appearance, then 1.0 s of background gray, (rectangular-wave, appearance-disappearance modulation) resulting in a period of 2.0 s, frequency 0.5 Hz, and duty cycle 25%.

Stimulus presentation was controlled using the Psychophysics Toolbox extensions (Brainard, 1997; Pelli, 1997; Kleiner et al., 2007) for Matlab R2012b, detailed in Nunez et al. (2017).

2.4. Heterochromatic flicker photometry

The equiluminance of each stimulus color compared to the background gray was determined for each participant with heterochromatic flicker photometry (HFP). A central color square or color-gray checkerboard of the same size and spatial frequency as the stimuli (but not fading to background) was exchanged with background at a frequency of 15 Hz. The radiance of the color which produced minimum flicker was recorded and averaged over 12 repeats to determine the luminance match.

2.5. Procedure

During each experiment the participant was seated such that their eye level was aligned with the center of the screen and the viewing distance was 114 cm. Stimuli were viewed binocularly. There was one block of 30 stimulus presentations for each pattern, color direction and cone-contrast combination; blocks were presented in random order. Each participant was asked to focus on the center of the screen, and to blink as little as possible, particularly when a stimulus was visible on the screen.

2.6. Data acquisition and analysis

Data were recorded using a BioSemi ActiveTwo system (BioSemi, Amsterdam, Netherlands) as detailed previously (Nunez et al., 2017). The trigger and EEG signals were sampled at a frequency of 2048 Hz,

with an open passband from 0 to 400 Hz. The topography of the cVEP for a participant viewing a color checkerboard is presented in Fig. 4 of Nunez et al. (2017), where the cVEP was confined in space on the scalp to the most posterior electrodes over V1 cortex. All the data reported in this paper were measured at electrode Oz, corresponding to the largest cVEP responses (Nunez et al., 2017).

Please see Nunez et al. (2017) for details of the analysis pipeline. Data were separated into trials containing a pre-stimulus period of 100 ms and post-stimulus period of 1000 ms and were linearly detrended before being baseline-corrected with respect to the average voltage of the pre-stimulus period. However, four participants who blinked repeatedly after the stimulus disappeared had their post-stimulus period restricted to the 500 ms when the stimulus was on-screen. Waveforms reconstructed from the inverse Discrete Fourier Transform were 60 Hz-notched for line noise and low-pass-filtered to 100 Hz.

3. Results

The experimental design was aimed to evoke responses only from visual neurons that responded to color, and to remove the possibility of luminance artifacts (Parry & Robson, 2012). We used HFP to ensure that each stimulus was equiluminant for each participant (see **Section 2.4**).

The experiments were also designed to evoke responses only from spatially-tuned, color-responsive neurons, the cells we have called double-opponent (Friedman et al., 2003; Johnson et al., 2001, 2004; Lennie et al., 1990; Livingstone & Hubel, 1984; Shapley et al., 2019; Thorell et al.,1984). Therefore, the stimuli of interest were fine, color checkerboard patterns on an equiluminant gray background. Checkerboards were used to produce a large cVEP. The human cVEP is known to be near maximal in amplitude for such spatial patterns (Rabin et al., 1994); the cVEP is much larger for a 3c/deg pattern than for a very low SF pattern or a large uniform field of color because the pattern cVEP amplitude is spatially bandpass in nature (Nunez et al., 2018; Rabin et al., 1994). Double-opponent cells in Macaque monkey cortex are also

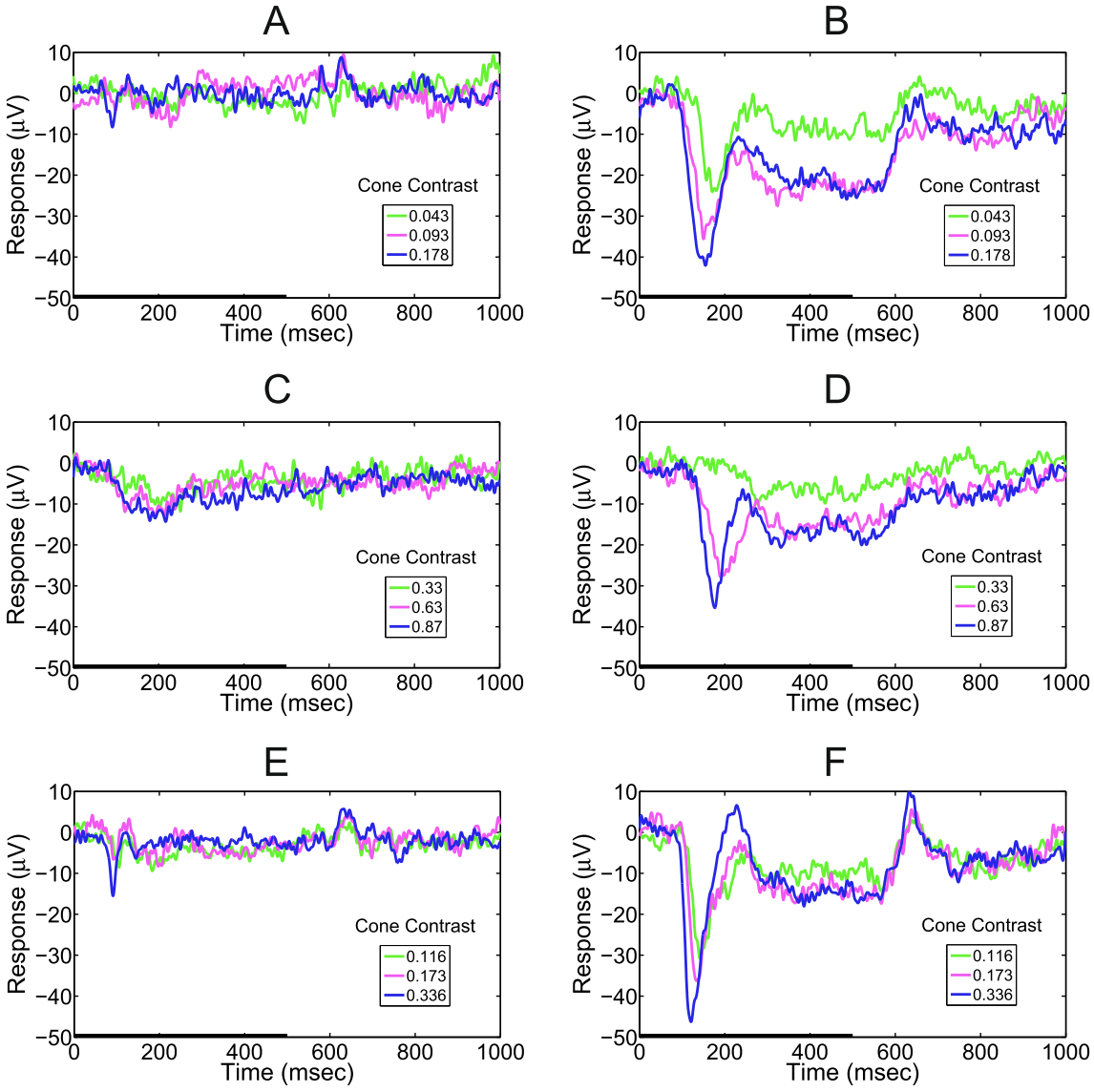

Fig. 3. The cVEP waveform at electrode Oz for one participant observing the (A) uniform square and (B) color-complement checkerboard patterns in the L-M color direction. For both stimuli, responses are plotted for a range of cone contrasts, covering the time period from pattern onset to 1000 ms after pattern onset. Note that the pattern was visible only for the first 500 ms, represented by the thick black bar along the time axis. C and D are the corresponding waveforms in the S-cone isolating direction. E and F are the corresponding waveforms in the Red direction. (For interpretation of the references to color in this figure legend, the reader is referred to the web version of this article.)

spatially-tuned for color, and they produce maximal visual responses for equiluminant color patterns around 2.6c/deg in SF (Johnson et al., 2001; Schluppeck & Engel, 2002). On the contrary, single-opponent neurons produce maximal visual responses around 0.5c/deg, with responses reduced by more than a factor of 20 around 3c/deg (Schluppeck & Engel, 2002). Therefore, single-opponent neurons should have minimal responses to the 3c/deg checkerboards used in these experiments.

Alternate checks in the color checkerboard stimuli were color-complements of each other so the energy spectrum of the spatially-averaged checkerboard was identical to that of the gray background. The checkerboard pattern consisted of a small, central colored checkerboard surrounded by an area in which the colored checks faded outwards gradually to the background gray (see **Section 2.3** for details). We restricted stimulus size to avoid contaminating the cVEP with luminance artifacts that might be caused by variation of spatio-chromatic responses with retinal eccentricity (Parry & Robson, 2012).

Uniformly-colored squares were used to compare cortical responses to areas of color with those of color-checkerboard patterns. As described in **Section 2.3**, the color squares were of the same spatial extent as the checkerboards with which they were compared, and were modulated in the same directions of color space (Fig. 1). We chose to describe chromatic modulation in terms of L-M and S-cone contrast for the L-M and S-cone isolating cardinal directions and in terms of the vector sum of the contrasts along the cardinal directions for the intermediate Red stimuli. Our logic for this was that it describes the magnitudes of the subcortical input to the cortex, and equalizing along the axes should equalize the inputs to the different pathways.

3.1. Individual cVEP waveforms

Waveforms of cVEP responses to the squares and checkerboards are presented in Fig. 3. Responses from one participant (P1), who viewed stimuli in all three color directions, are shown. The waveforms in Fig. 3 are for three cone contrast levels (low, medium and high) in each color direction. In the graphs, the color stimulus appeared from 0 to 500 ms on the time axis as indicated by the black bar at the bottom of each waveform plot, and the display screen returned to uniform gray after 500 ms.

The response to a large uniform square (see **Section 2.3**) is plotted in panels A, C, E, and the response to checkerboards in panels B, D, F, all on the same scale. That the responses are much larger for the color patterns than for a spatially-uniform field of color demonstrates that the cVEPs are the summed responses of populations of neurons that are spatially-tuned for color patterns. We also wish to point out that responses to stimulus offset are either not present or are opposite in sign to the onset responses, an indication that the onset peaks are not due to luminance artifacts, according to Robson, McKeefry, and Kulikowski (1997).

3.1.1. cVEP waveforms in the L-M direction as a function of cone-contrast

First, we focus on cVEP responses when the stimulus color was modulated in the L-M cardinal direction of color space (Derrington et al., 1984). Alternating checks along a row or column of the color-complement checkerboards appeared either reddish (L-M) or greenish (M−L), as seen in the middle row of Fig. 1A.

The response to the large uniform square in Fig. 3A is small at all cone-contrasts. Previous studies of the spatial tuning of the cVEP also implied that responses to large uniform color modulation in the L-M color direction would be weak (Murray et al., 1987; Rabin et al., 1994) and Fig. 3A confirms that. The much larger cVEP in Fig. 3B had the well-known initial negative peak (Murray et al., 1987; Rabin et al., 1994; Souza et al., 2008; Crognale, 2002; Crognale et al., 2013) and then relaxed to a negative voltage that persisted until stimulus offset. Typically, the transient at stimulus onset was much larger than any transient at offset. The time-to-peak of the initial negative transient (Fig. 3B) was shorter as contrast increased, replicating results of earlier studies (Crognale et al., 1993; Crognale, Switkes, & Adams, 1997; Nunez et al., 2017; Rabin et al., 1994; Souza et al., 2008).

3.1.2. cVEP waveforms in the S direction as a function of cone-contrast

Waveforms of the cVEP evoked by S-cone-modulated stimuli are plotted in Fig. 3C and 3D. The cVEP response evoked by a spatially-uniform square modulated in the +S direction (Fig. 3C), with small responses at all cone-contrasts, replicates earlier work (Rabin et al., 1994). The larger checkerboard response (Fig. 3D) has an initial negative transient and a reduction in time-to-peak with increasing S-cone-contrast (Crognale et al., 1997). The resemblance between the S-driven and L-M waveforms is remarkable because the LGN inputs to the cortex for L-M and S-cone driven stimuli are completely different and independent: Parvocellular and Koniocellular afferents respectively (Casagrande, 1994; Chatterjee & Callaway, 2003).

For the S-cone-driven cVEP (Fig. 3D) to reach a maximum amplitude required about 5X as much cone-contrast as for the L-M driven cVEP (Fig. 3B). Psychophysical data have also shown weaker responses for S-cone contrast than L-M contrast: Cole, Hine and McIlhagga (1993) found that S-cone detection thresholds were much higher than L-M thresholds when each mechanism of the cardinal axes was assumed to be a linear sum of cone contrasts; and in an experiment where participants matched contrast sensation across color directions, Switkes and Crognale (1999) found that S-cone contrast was perceived as approximately 8 times weaker than L-M contrast.

3.1.3. cVEP waveforms in the Red direction as a function of cone-contrast

The cVEP responses of P1 to Red modulation are plotted in Fig. 3E and F. The cVEP to the uniform square was again small, consistent with previous results (Nunez et al., 2018, Fig. 3 in that paper). Similar to the L-M and S directions, Red-complement checkerboards have the same large negative transient peak early after stimulus onset, and exhibit a reduction of the time-to- peak as cone-contrast increases. However, there are quantitative differences; in particular, the Red responses in Fig. 3F at high cone-contrast relax to a smaller voltage response around 500 ms, near the end of the stimulus period, than the corresponding high-contrast L-M or S-driven responses in Fig. 3B and 3D. This is examined further in the **Section 3.2.4.**

3.2. Quantitative analysis of population data.

Next we focus on population responses for color-complement checkerboards in the different color directions. We analyzed peak amplitude (defined as magnitude of stimulus-evoked peak negativity minus the baseline before stimulus appearance) and also three measures of response dynamics. The first measure was latency, here defined as the time taken from stimulus onset to reach 75% of the peak amplitude. The second was full-width-at-half-maximum or FWHM. And the final measure of response dynamics was Transientness, which is a measure of how big the initial negative peak is compared to the ongoing negativity during the duration of the stimulus. We defined Transientness by Eq. (1):

$$\text{Transientness} = \frac{\left\{V(t_{peak}) - < V(t) >_{300-500ms}\right\}}{V(t_{peak})} \quad (1)$$

where $V(t_{peak})$ = peak amplitude and $< V(t)>_{300–500ms}$ = average amplitude 300–500 ms after stimulus onset.

We chose to use separate t-tests to compare two color directions at a time because while all 7 of the participants who viewed the L-M stimuli had also viewed the S stimuli, of the 13 sets of usable data in the Red color direction, only four participants had also viewed the L-M and S stimuli. Therefore, when comparing L-M and S means, we used the paired *t*-test for the 7 participants, but when comparing Red with L-M or S we used the revised t-statistic of Derrick et al. (2017) which was created specifically for partially overlapping data. The revised t-statistic of Derrick et al. (2017) acts as a linear interpolation between the paired-samples and independent-samples t-tests, and has high Type I error

robustness, but also increased power due to using all the available data.

3.2.1. cVEP amplitudes vs cone-contrast

Median cVEP amplitudes are plotted vs stimulus contrast (Fig. 4). The dotted lines indicate upper and lower quartiles of the distribution of amplitudes across the population of participants. We used one x-axis coordinate for the cone-contrast in the three color-directions: the magnitude of the vector sum $\sqrt{(|L\text{-}M|^2+|S|^2)}$. For stimuli in the L-M direction, S = 0, and so for those stimuli, $\sqrt{(|L\text{-}M|^2+|S|^2)} = |L\text{-}M|$. For stimuli in the S-cone cardinal direction (L-M) = 0; for those stimuli, $\sqrt{(|L\text{-}M|^2+|S|^2)} = |S|$. For stimuli in the Red direction, contrast in both cardinal directions varied and the effective contrast was the magnitude of the vector sum of the contrasts along the cardinal directions.

The cVEP amplitude vs. cone-contrast data tell a lot about color signals in the early visual cortex. Consider L-M contrast first. Response amplitudes are quite large even at low contrast. We can calculate the (median) contrast gain for the L-M responses by computing the slope of the line connecting the origin to the median response at the lowest contrast with a response (see Kaplan & Shapley, 1986), which for L-M is 0.043. The contrast gain computed in this way is = 16 μV/0.043 = 372 μV/(unit contrast). However, L-M response amplitude saturates at fairly low L-M contrast. The median amplitude grows by about 25% over the range (0.05–0.25) where L-M contrast increases by 500%. This response saturation is one sign of nonlinear cortical interactions. Another indication of nonlinearity is that when we try to fit a straight line to the medians of L-M amplitude data as shown in Fig. 4, the fit is poor, especially at lower contrast. For the best fit line, the value of $R^2 = 0.65$, as a consequence of amplitude saturation for contrasts > 0.05. For Red, as for L-M, our attempt to fit the medians of response amplitude with a straight line is not very successful. The value of R^2 for the best fit line is 0.73. As in the case of modulation in the L-M direction, it is as if there is a steep early portion of the amplitude vs contrast curve which then curves into a line of shallower slope for Red contrast > 0.03.

S-cone stimuli evoke responses of much smaller amplitude than L-M or Red (Fig. 4) at the same cone contrast. For instance, at cone contrast = 0.2, the median S-cone-driven response is 6 μV (by interpolation in Fig. 4), while the median L-M response is approximately 22 μV. The contrast gain for the S-cone-driven cVEP is much smaller (=11 μV/0.33 = 33 μV/(unit contrast)) —approximately 10X smaller than for L-M signals. It is worth noting that the cVEP amplitude at the highest contrast in the S-direction is only a little smaller than the amplitude of the cVEPs evoked by the highest attainable L-M contrast. However, maximal S-cone-driven responses are considerably smaller than the largest Red responses (Fig. 4).

The response amplitudes to S-cone stimuli suffer less saturation than response amplitudes to L-M or Red stimuli. This follows from the good fit of a straight line to the amplitudes of S-cone-driven cVEP data (Fig. 4): $R^2 = 0.94$. In terms of cVEP amplitude vs cone-contrast, the S-cone pathway is more linear than L-M or Red. The linearity of the S-cone amplitudes enables the S-cone-driven responses to catch up, almost, to the maximum amplitude of the L-M and Red directions, at very high S-cone-contrast (Fig. 4). However, Rabin et al. (1994) observed response saturation for S-cone stimuli with a grating of spatial frequency 1c/deg. As that would have been closer to the optimal spatial frequency for the S direction it is possible that the lack of saturation in the S-direction is not intrinsic to cortical pathways but instead is due to stimulus conditions.

3.2.2. Latency

The latency of the cVEP waveform is a useful measure of response dynamics. In the present study, we found that latency is much shorter at higher cone contrast in all measured directions of color space (Fig. 5), replicating previous results (Murray et al., 1987; Nunez et al., 2017; Rabin et al., 1994; Souza et al., 2008; Crognale et al., 2013). The L-M and Red latencies averaged over all participants were almost identical (Fig. 5). The average latency of the S-cone-driven cVEP was much larger, also replicating prior results (Crognale et al., 2013; Rabin et al., 1994; see also Cottaris & DeValois, 1998 for uniform field stimuli).

In Fig. 5, at the highest possible contrast in each direction, the latencies are 109 ms for L-M, 116 ms for Red, and 151 ms for S. However, one needs to be cautious about interpreting this result as meaning that the S-cone-driven responses in V1 are ~40 ms slower for S than for L-M. That statement is correct for the conditions of our experiments in which the spatial patterns were the same for all color directions. However, the optimal spatial pattern for S-cone responses is likely to be lower in fundamental spatial frequency (larger check size) than for L-M or Red, and the corresponding S-cone-driven latency might be less for a spatially coarser pattern (Rabin et al., 1994). We are now investigating the open question: how does the shortest latency for cVEP responses to S-cone-driven stimuli compare to the shortest latency that L-M stimuli can evoke, when stimuli are spatial-frequency-optimized in each color direction?

Response latencies in each color direction decreased with increasing cone-contrast. This is a dynamic nonlinearity of color signal processing introduced in the cortex (see **Section 4.3**). The data summarized in Fig. 5 establish that the same kind of dynamic nonlinearity speeds up L-M, Red, and S-cone -driven responses. Thus, even though the path of S-cone signals into V1 cortex is different from that of L-M signals (Chatterjee & Callaway, 2003), within the cortex both kinds of color signals are altered dynamically in a similar manner as cone-contrast increases.

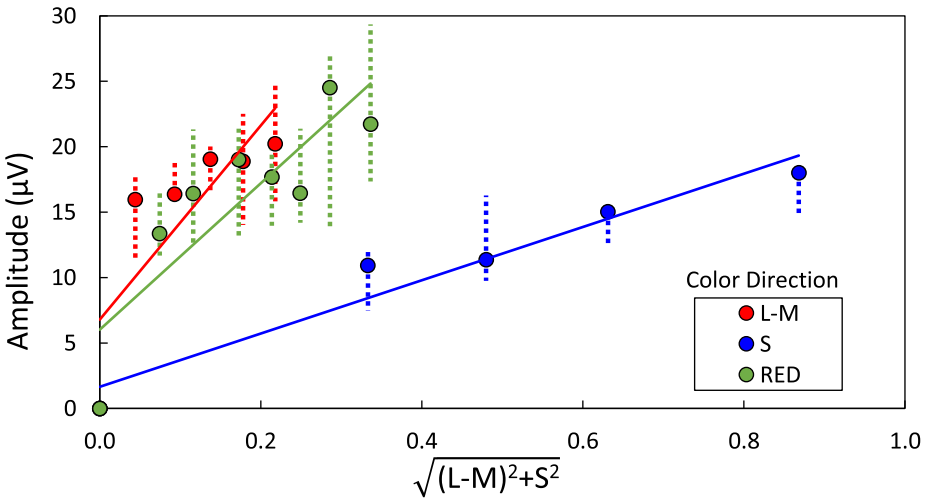

Fig. 4. Median Peak Amplitude of the participants plotted as a function of contrast measure for the color-complement stimuli in the three different color directions. For the L-M color direction, the effective contrast was |L-M|, for the RED color direction $\sqrt{(L\text{-}M)^2 + S^2}$ and for the S-cone direction |S|. The interquartile range of each data point is represented by dashed lines. As the peak is negative (Fig. 3), the absolute value of the peak response was used as the amplitude. A value of zero response at zero contrast was added for each color direction. Trend lines were fitted through each set of data using the method of least squares. (For interpretation of the references to color in this figure legend, the reader is referred to the web version of this article.)

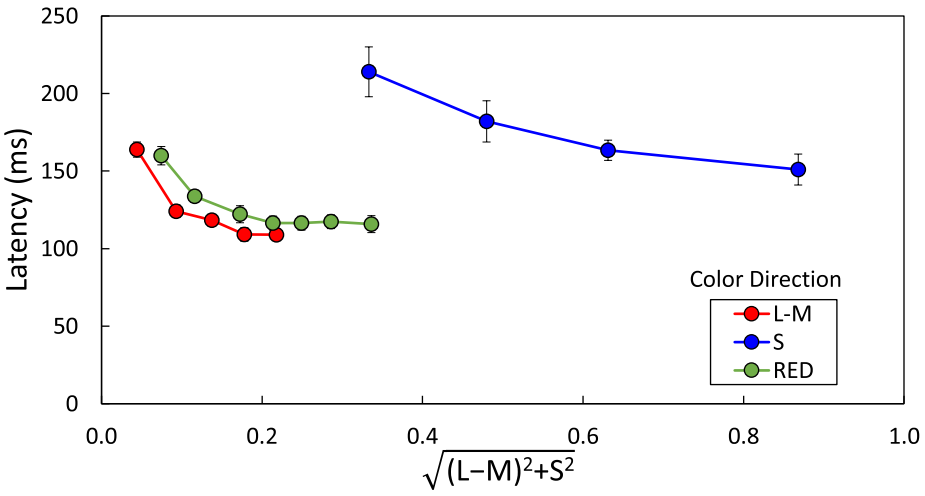

Fig. 5. Mean latency plotted as a function of a cone-contrast measure for the color-complement stimuli in the three different color directions. Latency was defined as the time taken from stimulus onset to reach 75% of the peak amplitude of response. For the L-M color direction, the effective contrast was |L-M|, for the RED color direction $\sqrt{(\text{L-M})^2 + \text{S}^2}$, and for the S-cone direction |S|. Error bars represent ± 1 SEM. (For interpretation of the references to color in this figure legend, the reader is referred to the web version of this article.)

3.2.3. *Response width (FWHM)*

Another dynamic feature of the cVEP waveform is the width (FWHM) of the initial negative peak. In our earlier study (Nunez et al., 2017), we thought that the FWHM of cVEP responses in the Red direction became smaller with increasing Red contrast. However, with the present dataset, FWHM for the color-complement checkerboards does not vary significantly with contrast (Fig. 6) for any of the directions in color space we tested: Red, L-M or S-cone. Another feature of the data is the extensive overlap of values of FWHM for L-M and for Red stimuli across cone-contrast (Fig. 6) and on average.

There is a measurable difference between the contrast-averaged FWHM of Red and L-M on the one hand, and S on the other. While FWHM for L-M and Red were nearly the same, the average S-cone-driven FWHM was 11–13 ms wider. However, the differences between the FWHMs of the S direction and the L-M & Red directions were not statistically significant.

3.2.4. *Transientness*

The last statistic studied is what we called Transientness of the cVEP responses to the 0.5 sec steps of color contrast that comprised the visual stimuli. As seen in Fig. 3, the cVEP was a transient negative dip soon after the color pattern appeared, followed by a relaxation to a prolonged negativity that persisted while the pattern remained visible, and relaxation to baseline after the color pattern disappeared. From Eq. 1, when the sustained response equals the peak response, Transientness = 0. And when the sustained = 0, i.e., when the cVEP relaxes back to baseline before the end of the stimulus, then Transientness = 1.

There are two interesting results about Transientness comparisons in our data (Fig. 7A). One concerns the comparison between L-M and S in Transientness and the other is the comparison between L-M and Red. As in the previous figures, Fig. 7A shows the quantity of interest, in this case Transientness, as a function of cone-contrast. A 1-way ANOVA in each color direction indicated no significant effect of contrast in any of the color directions. Because there was little dependence of Transientness on cone contrast, we report contrast-averages of the Transientness of L-M, S, and Red in Fig. 7B.

First let's compare L-M and S directions. L-M and S responses are similar in Transientness across all cone-contrasts where responses are measurable (Fig. 7A). Comparing the contrast-averaged Transientness for the 7 participants who viewed both color directions (Fig. 7B), we find no significant difference between the L-M and S directions (Table 2). For both L-M and S responses the height of the sustained component of the cVEP was approximately 0.47 X the height of the early peak (Table 2). Such a finding is consistent with the idea that signals along the two cardinal directions experience similar signal processing.

However, the sustained response for Red was 0.3 X the peak

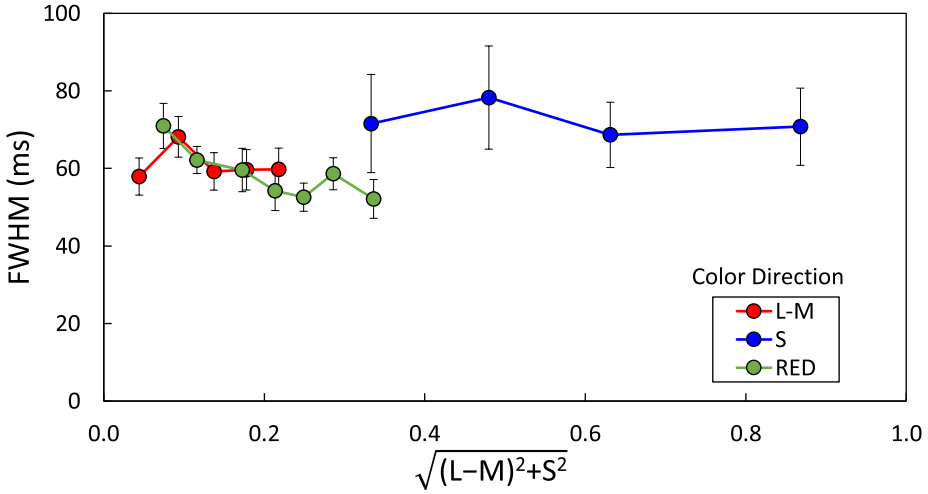

Fig. 6. Mean Full Width at Half Maximum (FWHM) plotted as a function of contrast measure for the color-complement stimuli in the three different color directions. For the L-M color direction, the effective contrast was |L-M|, for the RED color direction $\sqrt{(\text{L-M})^2 + \text{S}^2}$, and for the S-cone direction |S|. Error bars represent ± 1 SEM. (For interpretation of the references to color in this figure legend, the reader is referred to the web version of this article.)

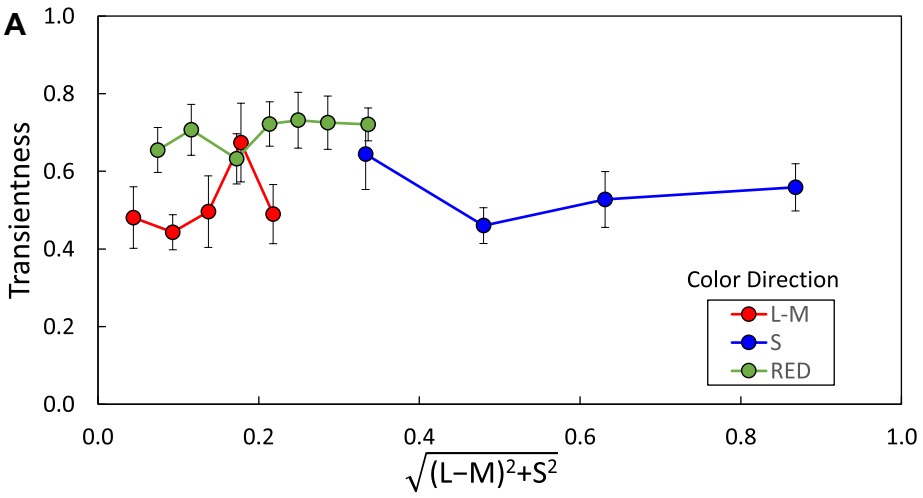

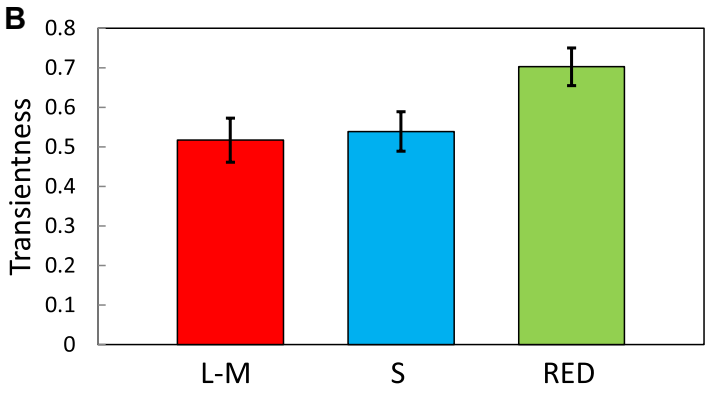

Fig. 7. A. Mean Transientness plotted as a function of contrast measure for the color-complement stimuli in the three different color directions. Transientness was defined as the difference between the peak amplitude and the average response over 300–500 ms post-stimulus, normalized by the peak amplitude. Error bars represent ± 1 SEM. B. Transientness averaged over each contrast range for the color-complement stimuli in the three different color directions. The contrast-averaged Transientness for each participant was converted to a grand average for each color direction. For the L-M and S directions, N = 7 and for the Red direction N = 13. Error bars represent ± 1 SEM. (For interpretation of the references to color in this figure legend, the reader is referred to the web version of this article.)

Table 2
Summary of *t*-test results comparing contrast-averaged Transientness in the L-M vs S, Red vs S, and Red vs L-M color directions. There was no significant difference in Transientness between the L-M and S directions, but Red Transientness was significantly larger than L-M and S Transientness.

Color direction	Mean Transientness	SEM	
L-M	0.52	0.06	
S	0.54	0.05	
RED	0.70	0.05	
Comparison of means	t-statistic	Degrees of freedom	p-value
L-M vs S	0.498	6	0.318
RED vs S	2.371	12	0.018
RED vs L-M	2.976	12	0.006

response. Responses in the Red direction have significantly higher Transientness than L-M or S (Table 2). This is also evident by comparing the waveforms in Fig. 3B, D, F. It is remarkable that the difference between Red and L-M is evident at even low cone contrast (Fig. 7A). At such low cone contrasts, the S-cone signal was too small to evoke measurable responses when presented alone (Fig. 3D). The difference in Transientness between Red and L-M directions is especially noticeable because Red and L-M did not differ significantly in peak height (Fig. 4), Latency (Fig. 5) or width (FWHM; Fig. 6). A prime topic of the **Discussion (Section 4)** must be what kind of mechanism could cause the difference in Transientness between Red and L-M and yet leave all the other measures the same in the two color directions. The fact that Transientness is greater for Red than for L-M suggests that the population of neurons that responds to Red may not be identical to the neural population responding to L-M.

4. Discussion

The cVEP signal represents the activity of a large population of neurons comprised of double-opponent color cells for the reason mentioned in **Section 1**: the cVEP is spatially-tuned (Murray et al., 1987; Rabin et al., 1994). One consequence of this population view is that the cVEP response to an L-M checkerboard pattern is coming from all V1 neurons that are responsive to L-M modulation. The same logic applies to responses to stimuli in the Red and S-cone-driven color directions. Based on what is known about the broad color tuning of most color-responsive neurons in Macaque V1 and V2 (Lennie et al., 1990; Kiper, Levitt, & Gegenfurtner, 2001), it is likely that many cortical neurons responded to checkerboard patterns in two or in all three of the color directions used in our experiments. The quantitative dynamical differences between cVEP responses to L-M, Red, and S-cone-driven stimuli must have resulted from different distributions of visually-evoked activity in the cortical network for different stimuli and not because one specifically tuned neuron-type was selected by the stimulus.

4.1. L-M vs S: parallel color pathways

The first comparison we will discuss is between effects of stimulation on V1 double-opponent populations in the L-M and S directions of color space. As presented in **Section 1**, L-M signals travel from eye to brain via P (midget) ganglion cells and Parvocellular LGN neurons (Lee, Martin, & Grünert, 2010; Chatterjee & Callaway, 2003). S-cone-driven signals are carried by SBS (Small-Bistratified) ganglion cells (Dacey & Lee, 1994) to the LGN, and by cells in the Koniocellular pathway to the cortex (Casagrande, 1994; Martin et al., 1997; Chatterjee & Callaway, 2003). These parallel retino cortical pathways are anatomically distinct. There

are many more Parvocellular (L-M) inputs to V1 than Koniocellular (S); in the central 10° of the visual field there are 5-10X as many P retinal ganglion cells as SBS cells (Dacey, 1994).

In Macaque V1, most double-opponent neurons that are S-cone-driven are also excited by L-M signals (Lennie et al., 1990; Johnson et al., 2004). Very few cells are found in V1 that respond to S-cone signals only. However, there are some double-opponent cells that appear to respond to color modulation in the L-M direction and receive no excitation from S-cones (Lennie et al., 1990; Johnson et al., 2004). The bottom line is that a larger fraction of the V1 population of double-opponent color cells is activated by L-M signals than by S-cone-driven signals. We can make estimates of the fractions of double-opponent cells in human V1 receiving inputs from the Parvo and Konio pathways using the cVEP data in this paper taken together with prior results on the visual responses of single cells in the two pathways.

The cVEP results on amplitude vs cone-contrast (Fig. 4) are consistent with the much smaller number of S-cone-driven inputs to V1 arriving via the Konicellular pathway. Much higher cone-contrast is required for S-cones to produce the same amplitude cVEP as L-M modulation. In **Section 3.2.1,** we calculated that contrast gain for S-cone-driven cVEPs is approximately 10X smaller than for L-M. However, single-cell studies of S-cones (Baudin et al., 2019), retinal ganglion cells (Yeh, Lee, & Kremers, 1995), and LGN cells (Tailby, Solomon, & Lennie, 2008), indicate that contrast gain in S-cones and S-cone-driven ganglion cells and LGN cells is not lower than in P cells and Parvocellular LGN cells. The lower contrast gain of S-cone-driven cVEPs therefore could reflect the smaller numbers of Konio inputs to V1. However, it may also reflect the fact that the stimulus spatial frequency was closer to optimal for the L-M than the S direction.

Even though the contrast gain of the S-cone-driven cVEP is ten times less than for L-M, the S-cone-driven cVEP amplitude at high contrast becomes comparable to that reached by L-M evoked signals (Fig. 4). This is because the amplitude of the S-cone-driven cVEP grows roughly proportional to cone contrast while the amplitude of the L-M-driven cVEP saturates at a low L-M contrast. The saturation of the L-M response at low contrast is not seen in responses of P ganglion cells (Yeh et al., 1995) and is likely caused by cortical interactions. The absence of saturation of the S-cone evoked signals could be caused either by a different amount of intracortical interactions or by greater recruitment at high contrast of neurons with weak S-cone inputs, or both. It is unlikely to be caused by differences in pre-cortical response vs contrast functions; the response vs contrast curves for P ganglion cells and Blue ON cells (almost certainly SBS cells, cf. Dacey & Lee, 1994) are quite similar (Yeh et al., 1995).

The dynamical difference in response latency (Fig. 5) between S-cone driven cVEPs and those evoked by L-M contrast are also likely to be caused by cortical mechanisms. The temporal impulse response of S-cones is reported to have a time-to-peak that is slightly (~10 ms) larger than for L or M cones (Baudin et al., 2019). However, time-to-peak of P ganglion cells and Blue ON cells, inferred from temporal frequency tuning curves, is the same (Yeh et al., 1995). The very large difference in latency between S and L-M cVEPS therefore is likely caused by cortical cell properties and/or cortical network interactions.

4.2. L-M vs Red: higher order color mechanisms

When we compare cVEPs to L-M and Red, the issues are different. There is no doubt that the two kinds of stimuli excite Parvocellular input to the cortex and that most or all of the cortical neurons that respond to Red also are excited by L-M stimuli. Rather, the question is, since Red stimuli contain both L-M and S-cone contrast (Table 1), is there any evidence that some part of the population of neurons responding to Red is comprised of neurons that combine L-M and S-cone signals, i.e., are there Higher Order Color Mechanisms in V1 (Krauskopf et al., 1986)?

The stimuli in the Red direction excited L, M and S cones. However, because of the low contrast gain of the S-cone signals, simple addition of the S- and L-M-evoked-cVEPs only would be expected to modify the response amplitude for Red stimuli with S-cone contrast > 0.2. There are increases of Red amplitudes above the saturated values of the L-M amplitudes at the two highest Red contrasts where S-cone-contrast > 0.2 (Fig. 4) which could be the evidence we seek for combination of L-M and S signals. Therefore, the first indication that there likely are Higher-Order neurons is the greater amplitude of Red over L-M responses at high contrast. However, in terms of contrast gain, latency, and response width (FWHM), cVEPs in the L-M and Red directions are quite similar.

More compelling evidence for Higher Order Color neurons that mix L-M and S signals is the pattern of the Transientness data. cVEP responses to Red are significantly more transient than to L-M. Since Red stimuli contain L-M and S contrast, simple summation of the L-M-driven and S-cone-driven cVEPS would result in a Red response that has equal or less Transientness than L-M alone but that is the opposite of what was observed. The greater transience of Red responses could be explained by antagonistic interactions within the cortex between L-M signals and S-cone signals in single cells that are elements of a population of Higher Order color neurons. Experimental data on populations of V1 color-responsive neurons, many of which combine L-M and S-cone signals (Lennie et al., 1990; Johnson et al., 2004), support the cVEP results. Note that comparisons of cVEP responses to objects and nonobjects (Martinovic, Mordal, & Wuerger, 2011) indicated less difference between responses for S and L-M & S stimuli than observed here. However, our Red was not the same mixture of L-M and S used by Martinovic, Mordal, and Wuerger (2011). They reported more Transientness when luminance was added to the L-M & S stimuli but that is not relevant to our results because we minimized luminance intrusion through the use of individual HFP.

4.3. Change of cortical dynamics with visual contrast

It is well-known that the dynamics of cVEPs vary with cone-contrast (Crognale et al., 1993; Nunez et al., 2017; Porciatti & Sartucci, 1996; Rabin et al., 1994; Souza et al., 2008). Here we observed that the contrast-dynamics effects are roughly similar for L-M, Red, and S-cone-only directions in color space. The effects of cone-contrast on the time course of responses of cells in the Parvocellular and Koniocellular pathways are much weaker than the very large effect of cone-contrast on latency shown in Fig. 5 (reviewed in Nunez et al., 2017). This indicates that the reduction in latency shown in Fig. 5 is a result of nonlinear cortical interactions, for instance a cortical contrast gain control, as proposed previously (Nunez et al., 2017). Recent theoretical work suggests that what is called cortical contrast gain control may be the result of recurrent excitatory and inhibitory interactions in the cortical network (Chariker, Shapley, & Young, 2020).

Our results on human cVEPs are consistent with a large body of research on color responses of neurons in primate V1 (Friedman et al., 2003; Johnson et al., 2001, 2004; Lennie et al., 1990; Livingstone & Hubel, 1984; Thorell et al., 1984). There appear to be many distinct populations of pattern-selective cortical neurons. Neurons in different populations combine signals from Parvocellular and Koniocellular sources with different weightings, and then interact with one another through recurrent excitatory and inhibitory interactions. Different stimuli, for example L-M vs Red, have different population activity profiles that are a result of these cortical neural computations. The cortical interactions lead to different dynamical signatures of the population responses that need to be determined in future research.

Funding

This project owes its support to the US National Science Foundation (grant number 1753846).

CRediT authorship contribution statement

Valerie Nunez: Conceptualization, Methodology, Software, Investigation, Data curation, Visualization, Formal analysis, Writing - original draft, Writing - review & editing. **James Gordon:** Project administration, Supervision, Resources, Conceptualization, Methodology, Investigation, Visualization, Formal analysis, Writing - review & editing. **Robert M. Shapley:** Funding acquisition, Project administration, Supervision, Resources, Conceptualization, Methodology, Investigation, Visualization, Formal analysis, Writing - original draft, Writing - review & editing.

Declaration of Competing Interest

The authors declare that they have no known competing financial interests or personal relationships that could have appeared to influence the work reported in this paper.

Acknowledgements

We wish to thank the following lab members who helped run the experiments: Afsana Amir, Chloe Brittenham, Syed Ali Hassan, Patricia Pehme, Vera Pertsovskaya, & Ashley Rosemond.

References

Baudin, J., Angueyra, J. M., Sinha, R., & Rieke, F. (2019). S-cone photoreceptors in the primate retina are functionally distinct from L and M cones. *eLife, 8*. https://doi.org/10.7554/eLife.39166.

Bimler, D. L., Paramei, G. V., & Izmailov, C. A. (2009). Hue and saturation shifts from spatially induced blackness. *Journal of the Optical Society of America A, Optics Image Science and Vision, 26*(1), 163–172. https://doi.org/10.1364/JOSAA.26.000163.

Bouet, R., & Knoblauch, K. (2004). Perceptual classification of chromatic modulation. *Visual Neuroscience, 21*(3), 283–289. https://doi.org/10.1017/S0952523804213141.

Bradley, A., Switkes, E., & DeValois, K. (1988). Orientation and spatial frequency selectivity of adaptation to color and luminance gratings. *Vision Research, 28*(7), 841–856. https://doi.org/10.1016/0042-6989(88)90031-4.

Brainard, D. (1996). Cone contrast and opponent modulation color spaces. In Kaiser, & Boynton (Eds.), *Human Color Vision* (pp. 563–579). Washington, DC: Optical Society of America.

Brainard, D. H. (1997). The Psychophysics Toolbox. *Spatial Vision, 10*(4), 433–436. https://doi.org/10.1163/156856897X00357.

Casagrande, V. A. (1994). A third parallel visual pathway to primate area V1. *Trends in Neurosciences, 17*(7), 305–310. https://doi.org/10.1016/0166-2236(94)90065-5.

Chariker, L., Shapley, R., & Young, L. S. (2020). Contrast response in a comprehensive network model of macaque V1. *Journal of Vision, 20*(4), 16. https://doi.org/10.1167/jov.20.4.16.

Chatterjee, S., & Callaway, E. M. (2003). Parallel colour-opponent pathways to primary visual cortex. *Nature, 426*(6967), 668–671. https://doi.org/10.1038/nature02167.

Cole, G. R., Hine, T., & Mcllhagga, W. (1993). Detection mechanisms in L-, M-, and S-cone contrast space. *Journal of the Optical Society of America A, 10*(1), 38–51. https://doi.org/10.1364/JOSAA.10.000038.

Conway, B. R., Chatterjee, S., Field, G. D., Horwitz, G. D., Johnson, E. N., Koida, K., & Mancuso, K. (2010). Advances in color science: From retina to behavior. *Journal of Neuroscience, 30*(45), 14955–14963. https://doi.org/10.1523/JNEUROSCI.4348-10.2010.

Cottaris, N. P., & DeValois, R. L. (1998). Temporal dynamics of chromatic tuning in macaque primary visual cortex. *Nature, 395*(6705), 896–900. https://doi.org/10.1038/27666.

Crognale, M. A. (2002). Development, maturation, and aging of chromatic visual pathways: VEP results. *Journal of Vision, 2*(6), 438–450. https://doi.org/10.1167/2.6.2.

Crognale, M. A., Switkes, E., & Adams, A. J. (1997). Temporal response characteristics of the spatio- chromatic visual evoked potential: Nonlinearities and departures from psychophysics. *Journal of the Optical Society of America A, 14*(10), 2595–2607. https://doi.org/10.1364/josaa.14.002595.

Crognale, M. A., Switkes, E., Rabin, J., Schneck, M. E., Hægerström-Portnoy, G., & Adams, A. J. (1993). Application of the spatiochromatic visual evoked potential to detection of congenital and acquired color-vision deficiencies. *Journal of the Optical Society of America A, 10*(8), 1818–1825. https://doi.org/10.1364/JOSAA.10.001818.

Crognale, M. A., Duncan, C. S., Shoenhard, H., Peterson, D. J., & Berryhill, M. E. (2013). The locus of color sensation: Cortical color loss and the chromatic visual evoked potential. *Journal of Vision, 13*(10), 15. https://doi.org/10.1167/13.10.15.

Dacey, D. M. (1994). Physiology, morphology and spatial densities of identified ganglion cell types in primate retina. *Ciba Foundation Symposium, 184*, 12–28. https://doi.org/10.1002/9780470514610.ch2.

Dacey, D. M., & Lee, B. B. (1994). The 'blue-on' opponent pathway in primate retina originates from a distinct bistratified ganglion cell type. *Nature, 367*(6465), 731–735. https://doi.org/10.1038/367731a0.

Derrick, B., Russ, B., Toher, D., & White, P. (2017). Test statistics for the comparison of means for two samples that include both paired and independent observations. *Journal of Modern Applied Statistical Methods, 16*(1), 137–157. https://doi.org/10.22237/jmasm/1493597280.

Derrington, A. M., Krauskopf, J., & Lennie, P. (1984). Chromatic mechanisms in lateral geniculate nucleus of macaque. *Journal of Physiology, 357*, 241–265. https://doi.org/10.1113/jphysiol.1984.sp015499.

DeValois, R. (1960). Color vision mechanisms in the monkey. *Journal of General Physiology, 43*(6), 115–128. https://doi.org/10.1085/jgp.43.6.115.

Duncan, C. S., Roth, E. J., Mizokami, Y., McDermott, K. C., & Crognale, M. A. (2012). Contrast adaptation reveals increased organizational complexity of chromatic processing in the visual evoked potential. *Journal of the Optical Society of America A, 29*(2), A152–A156. https://doi.org/10.1364/JOSAA.29.00A152.

Engel, S., Zhang, X., & Wandell, B. (1997). Colour tuning in human visual cortex measured with functional magnetic resonance imaging. *Nature, 388*(6637), 68–71. https://doi.org/10.1038/40398.

Faul, F., Ekroll, V., & Wendt, G. (2008). Color appearance: the limited role of chromatic surround variance in the "gamut expansion effect". *Journal of Vision, 8*(3), 30. https://doi.org/10.1167/8.3.30.

Friedman, H. S., Zhou, H., & von der Heydt, R. (2003). The coding of uniform colour figures in monkey visual cortex. *Journal of Physiology, 548*(2), 593–613. https://doi.org/10.1111/j.1469-7793.2003.00593.x.

Gegenfurtner, K. R., & Kiper, D. C. (1992). Contrast detection in luminance and chromatic noise. *Journal of the Optical Society of America A, 9*(11), 1880–1888. https://doi.org/10.1364/JOSAA.9.001880.

Highsmith, J., & Crognale, M. A. (2010). Attentional shifts have little effect on the waveform of the chromatic onset VEP. *Ophthalmological and Physiological Optics, 30*(5), 525–533. https://doi.org/10.1111/j.1475-1313.2010.00747.x.

Hurlbert, A., & Wolf, K. (2004). Color contrast: A contributory mechanism to color constancy. *Progress in Brain Research, 144*, 145–160. https://doi.org/10.1016/S0079-6123(03)14410-X.

Hurvich, L. M., & Jameson, D. (1957). An opponent-process theory of color vision. *Psychological Review, 64*(6p1), 384–404. https://doi.org/10.1037/h0041403.

Johnson, E. N., Hawken, M. J., & Shapley, R. (2001). The spatial transformation of color in the primary visual cortex of the macaque monkey. *Nature Neuroscience, 4*(4), 409–416. https://doi.org/10.1038/86061.

Johnson, E. N., Hawken, M. J., & Shapley, R. (2004). Cone inputs in macaque primary visual cortex. *Journal of Neurophysiology, 91*(6), 2501–2514. https://doi.org/10.1152/jn.01043.2003.

Kaplan, E., & Shapley, R. (1986). The primate retina contains two types of ganglion cells, with high and low contrast sensitivity. *Proceedings of the National Academy of Sciences, 83*(8), 2755–2757. https://doi.org/10.1073/pnas.83.8.2755.

Kiper, D. C., Levitt, J. B., & Gegenfurtner, K. R. (2001). Chromatic signals in extrastriate areas V2 and V3. In K. R. Gegenfurtner, & L. T. Sharpe (Eds.), *Color Vision, from genes to perception* (pp. 249–268). Cambridge: Cambridge University Press.

Kleiner, M., Brainard, D., Pelli, D., Ingling, A., Murray, R., & Broussard, C. (2007). What's new in Psychtoolbox-3. *Perception, 36*(1), 1–16.

Kleinschmidt, A., Lee, B. B., Requardt, M., & Frahm, J. (1996). Functional mapping of color processing by magnetic resonance imaging of responses to selective P- and M-pathway stimulation. *Experimental Brain Research, 110*, 279–288. https://doi.org/10.1007/BF00228558.

Krauskopf, J., & Gegenfurtner, K. (1992). Color discrimination and adaptation. *Vision Research, 32*(11), 2165–2175. https://doi.org/10.1016/0042-6989(92)90077-V.

Krauskopf, J., Williams, D. R., & Heeley, D. W. (1982). Cardinal directions of color space. *Vision Research, 22*(9), 1123–1131. https://doi.org/10.1016/0042-6989(82)90077-3.

Krauskopf, J., Williams, D. R., Mandler, M. B., & Brown, A. M. (1986). Higher order color mechanisms. *Vision Research, 26*(1), 23–32. https://doi.org/10.1016/0042-6989(86)90068-4.

Lee, B. B., Martin, P. R., & Grünert, U. (2010). Retinal connectivity and primate vision. *Progress in Retinal Eye Research, 29*(6), 622–639. https://doi.org/10.1016/j.preteyeres.2010.08.004.

Lennie, P., Krauskopf, J., & Sclar, G. (1990). Chromatic mechanisms in striate cortex of ma- caque. *Journal of Neuroscience, 10*(2), 649–669. https://doi.org/10.1523/JNEUROSCI.10-02-00649.1990.

Livingstone, M. S., & Hubel, D. H. (1984). Anatomy and physiology of a color system in the primate visual cortex. *Journal of Neuroscience, 4*(1), 309–356. https://doi.org/10.1523/JNEUROSCI.04-01-00309.1984.

MacLeod, D. I., & Boynton, R. M. (1979). Chromaticity diagram showing cone excitation by stimuli of equal luminance. *Journal of the Optical Society of America, 69*(8), 1183–1186. https://doi.org/10.1364/JOSA.69.001183.

Martin, P. R., White, A. J. R., Goodchild, A. K., Wilder, H. D., & Sefton, A. E. (1997). Evidence that blue-on cells are part of the third geniculocortical pathway in primates. *European Journal of Neuroscience, 9*(7), 1536–1541. https://doi.org/10.1111/j.1460-9568.1997.tb01509.x.

Martinovic, J., Mordal, J., & Wuerger, S. M. (2011). Event-related potentials reveal an early advantage for luminance contours in the processing of objects. *Journal of Vision, 11*(7), 1. https://doi.org/10.1167/11.7.1.

Mullen, K. T., Dumoulin, S. O., McMahon, K. L., de Zubicaray, G. I., & Hess, R. F. (2007). Selectivity of human retinotopic visual cortex to S-cone-opponent, L/M- cone-opponent and achromatic stimulation. *European Journal of Neuroscience, 25*(2), 491–502. https://doi.org/10.1111/j.1460-9568.2007.05302.x.

Murray, I. J., Parry, N. R. A., Carden, D., & Kulikowski, J. J. (1987). Human visual evoked- potentials to chromatic and achromatic gratings. *Clinical Vision Sciences, 1*(3), 231–244.

Nunez, V., Shapley, R. M., & Gordon, J. (2017). Nonlinear dynamics of cortical responses to color in the human cVEP. *Journal of Vision, 17*(11), 9. https://doi.org/10.1167/17.11.9.

Nunez, V., Shapley, R. M., & Gordon, J. (2018). Cortical double-opponent cells in color perception: Perceptual scaling and chromatic visual evoked potentials. *i-Perception, 9*(1). https://doi.org/10.1177/2041669517752715.

Parry, N. R. A., & Robson, A. G. (2012). Optimization of large-field tritan stimuli using concentric isoluminant annuli. *Journal of Vision, 12*(12), 11. https://doi.org/10.1167/12.12.11.

Pelli, D. G. (1997). The VideoToolbox software for visual psychophysics: Transforming numbers into movies. *Spatial Vision, 10*(4), 437–442. https://doi.org/10.1163/156856897X00366.

Porciatti, V., & Sartucci, F. (1996). Retinal and cortical evoked responses to chromatic contrast stimuli: Specific losses in both eyes of patients with multiple sclerosis and unilateral optic neuritis. *Brain, 119*(3), 723–740. https://doi.org/10.1093/brain/119.3.723.

Rabin, J., Switkes, E., Crognale, M., Schneck, M. E., & Adams, A. J. (1994). Visual evoked potentials in three-dimensional color space: Correlates of spatio-chromatic processing. *Vision Research, 34*(20), 2657–2671. https://doi.org/10.1016/0042-6989(94)90222-4.

Robson, A. G., McKeefry, D. J., & Kulikowski, J. J. (1997). Visual evoked potentials: Special requirements for blue. In C. Dickinson, I. Murray, & D. Carden (Eds.), *John Dalton's Colour Vision Legacy* (pp. 115–123). London: Taylor and Francis.

Schluppeck, D., & Engel, S. A. (2002). Color opponent neurons in V1: A review and model reconciling results from imaging and single-unit recording. *Journal of Vision, 2*(6), 5. https://doi.org/10.1167/2.6.5.

Shapley, R., Nunez, V., & Gordon, J. (2019). Cortical double-opponent cells and human color perception. *Current Opinion in Behavioral Sciences, 30*, 1–7. https://doi.org/10.1016/j.cobeha.2019.04.001.

Souza, G. S., Gomes, B. D., Lacerda, E. M. C., Saito, C. A., da Silva Filho, M., & Silveira, L. C. L. (2008). Amplitude of the transient visual evoked potential (tVEP) as a function of achromatic and chromatic contrast: Contribution of different visual pathways. *Visual Neuroscience, 25*(3), 317–325. https://doi.org/10.1017/S0952523808080243.

Switkes, E., Bradley, A., & DeValois, K. K. (1988). Contrast dependence and mechanisms of masking interactions among chromatic and luminance gratings. *Journal of the Optical Society of America A, 5*(7), 1149–1162. https://doi.org/10.1364/JOSAA.5.001149.

Switkes, E., & Crognale, M. A. (1999). Comparison of color and luminance contrast: Apples versus oranges? *Vision Research, 39*(10), 1823–1831. https://doi.org/10.1016/S0042-6989(98)00219-3.

Tailby, C., Solomon, S. G., & Lennie, P. (2008). Functional asymmetries in visual pathways carrying S-cone signals in macaque. *Journal of Neuroscience, 28*(15), 4078–4087. https://doi.org/10.1523/JNEUROSCI.5338-07.2008.

Thorell, L. G., DeValois, R. L., & Albrecht, D. G. (1984). Spatial mapping of monkey VI cells with pure color and luminance stimuli. *Vision Research, 24*(7), 751–769. https://doi.org/10.1016/0042-6989(84)90216-5.

Victor, J. D., Maiese, K., Shapley, R., Sidtis, J., & Gazzaniga, M. S. (1989). Acquired central dyschromatopsia: Analysis of a case with preservation of color discrimination. *Clinical Vision Sciences, 4*(3), 183–196.

Wandell, B. A., & Winawer, J. (2011). Imaging retinotopic maps in the human brain. *Vision Research, 51*(7), 718–737. https://doi.org/10.1016/j.visres.2010.08.004.

Webster, M. A., & Mollon, J. D. (1994). The influence of contrast adaptation on color appearance. *Vision Research, 34*(15), 1993–2020. https://doi.org/10.1016/0042-6989(94)90028-0.

Xing, D., Ouni, A., Chen, S., Sahmoud, H., Gordon, J., & Shapley, R. (2015). Brightness–color interactions in human early visual cortex. *Journal of Neuroscience, 35*(5), 2226–2232. https://doi.org/10.1523/JNEUROSCI.3740-14.2015.

Yeh, T., Lee, B. B., & Kremers, J. (1995). Temporal response of ganglion cells of the macaque retina to cone-specific modulation. *Journal of the Optical Society of America A Optics and Image Science and Vision, 12*(3), 456. https://doi.org/10.1364/JOSAA.12.000456.

Zeki, S. (1983). Colour coding in the cerebral cortex: The reaction of cells in monkey visual cortex to wavelengths and colours. *Neuroscience, 9*(4), 741–765. https://doi.org/10.1016/0306-4522(83)90265-8.